ARTICLE

Check for updates

Snowfall-albedo feedbacks could have led to deglaciation of snowball Earth starting from mid-latitudes

Philipp de Vrese [1✉], Tobias Stacke [2], Jeremy Caves Rugenstein [3], Jason Goodman[4] & Victor Brovkin [1,5]

Simple and complex climate models suggest a hard snowball – a completely ice-covered planet – is one of the steady-states of Earth's climate. However, a seemingly insurmountable challenge to the hard-snowball hypothesis lies in the difficulty in explaining how the planet could have exited the glaciated state within a realistic range of atmospheric carbon dioxide concentrations. Here, we use simulations with the Earth system model MPI-ESM to demonstrate that terminal deglaciation could have been triggered by high dust deposition fluxes. In these simulations, deglaciation is not initiated in the tropics, where a strong hydrological cycle constantly regenerates fresh snow at the surface, which limits the dust accumulation and snow aging, resulting in a high surface albedo. Instead, comparatively low precipitation rates in the mid-latitudes in combination with high maximum temperatures facilitate lower albedos and snow dynamics that – for extreme dust fluxes – trigger deglaciation even at present-day carbon dioxide levels.

[1] Max Planck Institute for Meteorology, The Land in the Earth System, Hamburg, Germany. [2] Helmholtz-Zentrum Geesthacht, Institute of Coastal Research, Geesthacht, Germany. [3] Colorado State University, Department of Geosciences, Fort Collins, CO, USA. [4] Wheaton College, Department of Physics and Astronomy, Norton, MA, USA. [5] University of Hamburg, Center for Earth System Research and Sustainability, Hamburg, Germany. ✉email: philipp.de-vrese@mpimet.mpg.de

Whether our planet has ever been completely ice-covered has long fascinated geologists and climate modelers. Geological evidence suggests that Earth's past featured ice ages, during which the polar ice caps grew beyond the ice-albedo-instability threshold, triggering a runaway feedback that resulted in global glaciation—a state termed "snowball Earth"[1,2]. Two extraordinary glacial periods are thought to have occurred during the Neoproterozoic Era[1-8], but it remains a matter of debate whether these would have featured a complete ice cover, a so called "hard" snowball (HSB), or whether parts of the oceans remained ice free—a state often referred to as a "waterbelt"[9-12]. On one hand, certain factors—such as the survival of photoautotrophic organisms or large-scale basin-filling sedimentary patterns—are harder to explain in the context of a complete glaciation[2]. On the other hand, energy balance models, as well as intermediate- and full-complexity climate models agree that an HSB is indeed one of Earth's equilibrium states[13-17], whereas it is vastly more difficult to maintain an extreme icehouse state that retains open ocean surfaces[17-22].

Possibly the largest obstacle for the HSB hypothesis lies in the difficulty in explaining how Earth could have left the snowball state once it had been established. Deglaciation is thought to have eventually occurred as the ice cover prevented silicate weathering and photosynthesis, causing volcanic emissions to raise the atmospheric CO_2 concentration (pCO_2) to a level that allowed the planet to leave the icehouse state[1]. However, it has been extremely difficult to simulate the onset of deglaciation under plausible conditions. This can partly be attributed to the specific characteristics of the atmosphere of snowball Earth, such as the nearly isothermal structure during winter and a low water vapor content that leads to a comparatively weak greenhouse effect[23-28]. But the most fundamental challenge for initiating the deglaciation of an ice-covered planet is posed by its surface albedo. The high reflectivity of ice and snow, which would have enabled snowball Earth in the first place, may have also prevented its surface from absorbing enough energy to initiate a terminal deglaciation.

In the following, we analyze simulations with the Earth system model MPI-ESM1.2 (ref. [29], "Methods—Model configuration") to investigate dust deposition fluxes as a potential cause for HSB deglaciation. First, we use the model in a setup with prescribed reflectivities, that are independent from the snow cover, to estimate the surface albedos that trigger deglaciation within a range of plausible pCO_2 ("Dependency of ablation rates on albedo and CO_2"). Then, we briefly discuss the processes that modulate the

albedo on an ice-covered planet ("Snowball albedo"), before using the MPI-ESM with interactive surface albedos--based on an adapted snow-albedo-scheme—to investigate if these mechanisms could have sustained sufficiently low albedos to deglaciate an HSB ("Thawing the snowball"). The key modifications to the MPI-ESM's snow-albedo-scheme enable the representation of a sustained dust accumulation due to variable deposition fluxes and separate the snowpack into a main layer and a top layer, each possessing its own thickness, cover fraction, age, and albedo ("Methods—Snow-albedo-scheme"). This allows a more accurate representation of the surface albedo of an HSB, where the reflectivity would have partly been determined by a thin layer of comparatively fresh snow, which partially covers a thicker layer of perennial snow, and whose optical properties and extent can vary substantially on short timescales. Our simulations with this adapted model confirm previous studies, showing that a sustained dust accumulation at the surface could indeed have allowed to escape the snowball state[30-33]. However, in contrast to previous findings our results indicate that deglaciation would not have been triggered in the tropics, where a strong hydrological cycle constantly regenerates fresh bright snow at the surface, but in the midlatitudes, where snowfall rates are notably lower.

Results and discussion

Dependency of ablation rates on albedo and CO_2. Plausible albedos on an HSB range between roughly 0.9, the albedo of fresh snow and precipitated salt, and 0.45, the albedo of sea ice[34-37]. In agreement with previous studies[17,21,27,38], our simulations with prescribed surface albedos show that ablation rates, and hence the CO_2-threshold for deglaciation, are very sensitive to this surface property, especially for higher values that are representative of extensive snow covers (Fig. 1). For albedos > 0.65, a tenfold increase in pCO_2 hardly increases the maximum ablation rates, while an albedo reduction of <0.1 increase them by up to two orders of magnitude. Only when the albedo approaches that of old snow or meteoric ice—an albedo < 0.65—do ablation rates become more sensitive to changes in pCO_2.

When ablation is driven exclusively by sublimation, the rates are extremely low and the simulated maximum sublimation minus precipitation rates (SMPRs) hardly surpass 100 mm year^{-1}. However, ablation rates increase substantially when snow and ice begin to melt and reach values far >1000 mm year^{-1}. This is sufficient to degrade even a thick ice cover within a matter of
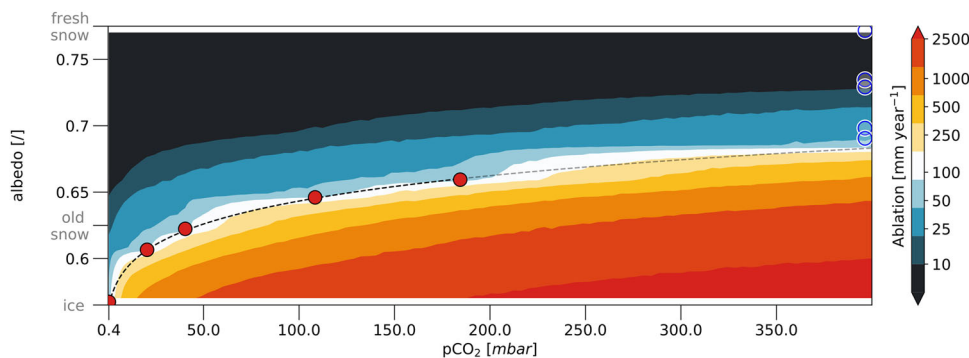

Fig. 1 Dependency of maximum ablation rates on surface albedo and atmospheric CO_2 concentrations. Simulated annual mean net ablation rates, that is the sum of sublimation and melt minus precipitation, as a function of atmospheric CO_2 concentration (pCO_2) and surface albedo (α). Rates show the average over the 18.75°-wide latitudinal band (~2000 km), in which maximum ablation rates were simulated. Values are interpolated between 10 simulations with the MPI-ESM1.2 (ref. [29]), in which the reflectivly of the surface was prescribed ("Methods—Model configuration, Simulations" and Supplementary Fig. 1). Red circles mark combinations of α and pCO_2 that resulted in simulated surface temperatures reaching the melting point, which is often considered the onset of deglaciation[23]. The dashed line shows a simple fit for albedo values that resulted in melt: $\alpha_{melt} \approx 0.0059 \cdot \ln(pCO_2)^{1.65} + 0.57$. Open circles to the far right show albedo values for which no deglaciation was simulated for CO_2 concentrations ≤ 400 mbar.

millennia, given that meltwater escapes the surface via (hydro-) fractures, moulins and supraglacial stream networks[39–43]. Triggering deglaciation within the geologically feasible pCO_2 range ($\lesssim 100$ mbar[2,44]) requires surface albedos of <0.65 (Fig. 1), which raises the question if such a low albedo could have been established and sustained on an HSB.

Snowball albedo. The surface albedo of a fully glaciated planet is largely determined by the reflectively and extent of the snow cover. Freshly deposited snow possesses an albedo of ~0.85, too high a value to render deglaciation possible (given that a significant fraction of the surface is covered with snow). However, the albedo decreases over time which is mainly due to structural changes within the snowpack, in which vapor diffusion increases the snow grain size close to the surface[45,46]. In addition, the snow albedo is reduced by the increasing concentration of impurities, resulting from the continuous deposition of dust particles at the surface. These processes, often referred to as snow aging, reduce the snow albedo to values <0.6[35], which is sufficiently low to sustain the deglaciation of an HSB. Here, the most prominent hypothesis for HSB deglaciation argues that the tropics featured a particularly low albedo—making it the region where deglaciation would have started—due to additional mechanisms that increase the surface dust concentration in ablation zones[30–33]. While ablation is driven by sublimation, it is reasonable to assume that degrading snow and ice leave behind the embedded particles, which would have accumulated at the surface. This process could have been supported by "viscous sea glacier flow"[47] laterally transporting the dust embedded within (sea) glaciers from the accumulation—to the ablation regions, where the degradation of the ice cover would have caused the dust to resurface ("sea ice elevator"[48]).

Notwithstanding the above processes, the albedo on an HSB would not necessarily have decreased to values low enough to initiate deglaciation. All sublimated water returns to the surface eventually, with precipitation regenerating fresh, bright snow at the surface. This snowfall-albedo feedback counteracts the effects due to aging and stabilizes the snow albedo, potentially at values that prevented deglaciation (Fig. 2). The hydrological cycle on a glaciated planet is never fully inactive, with the characteristic precipitation and sublimation patterns being very similar among the models that have been used in studies of snowball Earth[28,30,49]. Here, the tropics—between 10°N and 10°S—constitute the main ablation zone with sublimation outweighing the precipitation rates during the largest part of the year (Fig. 3). However, even during the (boreal) winter and summer season not all of the sublimated water is advected into the extratropics, and this fraction is almost negligible during spring and fall. Thus, fresh snow is constantly being regenerated at the surface within the tropics and only north of 30°N and south of 30°S does precipitation cease entirely during certain months.

The year-round precipitation in the tropics constitutes a crucial element of the HSB's hydrological cycle, because it means that even the main ablation zone did not necessarily feature the low albedo of exposed—potentially dust covered—(sea) ice. Rather than being snow free, the surface in the tropics would have been partly covered by a regenerative fresh-snow-layer at any given point in time. Snowfall rarely leads to a uniform, area-wide snow layer on the ground[35,50–52] and, on a fully glaciated planet, there would have been sublimation from patches of fresh snow, as well as from the snow-free adjacent areas. Under these circumstances, the snow cover reaches an extent that allows its mass loss due to sublimation to be completely balanced by snowfall. Hence, on shorter timescales, the position, size, and depth of individual snow patches would have varied substantially, but over longer
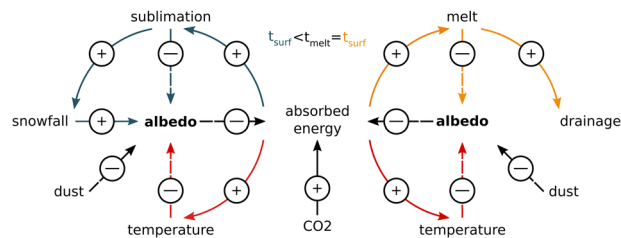

Fig. 2 Surface albedos on a hard snowball. Positive (solid lines) and negative (dashed lines) feedbacks between surface albedo, atmospheric CO_2 concentrations (pCO_2s), dust deposition fluxes, sublimation, melt, and snowfall. Blue colors pertain to the hydrological feedbacks for temperatures below the melting point, while yellow colors refer to feedbacks at the melting point. On an HSB, the surface albedo is largely determined by the albedo and extent of the snow cover. The snow albedo decreases due to snow aging, while snowfall (partly) restores it to the values of fresh bright snow. Here, the rate of decrease depends on the surface temperature and the dust deposition rates, with higher temperatures and dust fluxes accelerating snow aging. Furthermore, the surface albedo is reduced by sublimation and melt, because these diminish the snow cover, exposing more of the underlying darker surface. The temperature dependency of the above processes, leads to a lower albedo in ablation regions and an albedo decrease with rising pCO_2s. However, as long as temperatures stay below the melting point, the sublimated water will precipitate eventually, stabilizing the snow albedo and cover fraction, especially in regions with high and frequent precipitation. As precipitation also increase with higher pCO_2s, the rise in snowfall could potentially offset the effects due to accelerated snow aging at higher temperatures. When temperatures reach the melting point this negative snowfall-albedo feedback is eliminated because the meltwater drains from the surface and there is no link between melt and precipitation.

periods the snow cover fraction would have been proportional to the ratio of precipitation and sublimation (P/S ratio, Fig. 4). This equilibrium of the snow cover exists as long as temperatures stay below the melting point. Once melting is triggered the snowfall-albedo feedback is eliminated, because the meltwater drains without affecting precipitation. Here, several studies have argued that, over the duration of a snowball event, dust accumulation in the tropics could have resulted in a thick dust layer that would have inhibited sublimation and lowered albedos to a level at which temperatures reach the melting point[30,32]. However, it is highly questionable whether a thick dust layer could have persisted after the onset of melting because the dust particles would have been washed away with the meltwater, resulting in a negative feedback termed the "dust thermostat"[33].

Thawing the snowball. Considering the above processes, the feasibility of HSB deglaciation depends largely on the dust deposition rates, the planet's hydrological cycle, and the resulting snow dynamics. If aging and ablation reduced the snow albedo and cover sufficiently, deglaciation would have been possible within the plausible pCO_2 range, but if the snowfall-albedo feedback had been strong enough to maintain high surface albedos, Earth would have stayed in the snowball state indefinitely. Here, our simulations with an interactive surface albedo demonstrate that the deglaciation of an HSB would have generally been possible, if dust deposition fluxes had been high enough. However, contrary to the prevailing theory, our results indicate that it would not have been initiated in the tropical ablation zone.

Tropical SMPRs stay well <100 mm year^{-1}, even for dust deposition rates that are twice as large as the present-day values, and melting is not triggered within the reasonable pCO_2 range (Fig. 5a). These ablation rates would not have been sufficient to
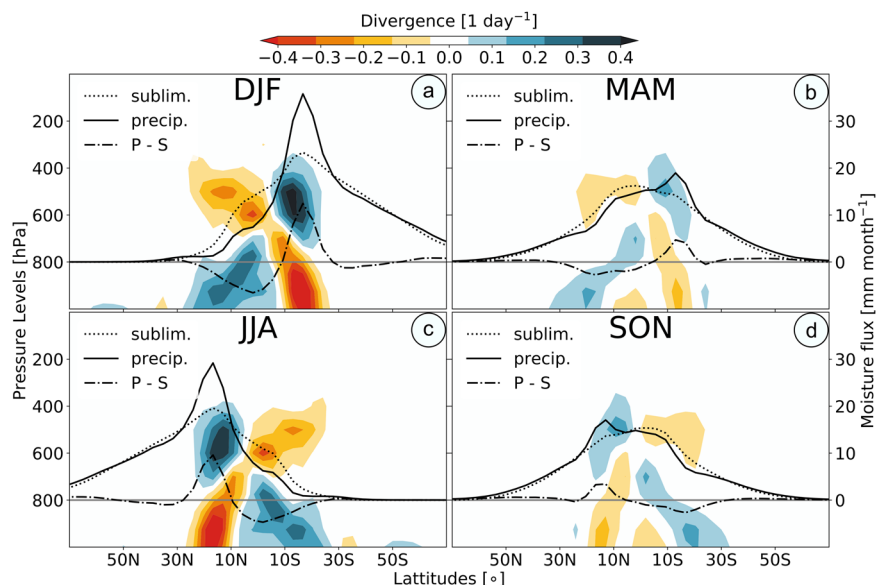
Fig. 3 Atmospheric dynamics on an HSB approaching deglaciation. a Zonal mean divergence, precipitation (thick solid line), sublimation (dotted line), and precipitation–sublimation rates (dashdotted line) averaged over the the period December—February, simulated with a prescribed surface albedo of 0.66 and atmospheric CO_2 concentrations of 100 mbar. **b** Same as **a** but for March–May. **c** Same as **a** but for June–August. **d** Same as **a** but for September–November. When simulated with ECHAM6, the atmospheric dynamics of an HSB are comparable to those simulated with other GCMs[28], hence the resulting precipitation minus sublimation (P − S) patterns are also very similar. The center of the tropics, roughly between 10.0° N–10.0° S, constitutes a predominantly descending region and the sublimation fluxes are larger than the precipitation rates, while they are much smaller than the precipitation rates in the ascending regions between 10.0° N–20.0° N and 10.0° S–20.0° S. This results in the typical P − S pattern with the tropical ablation zone located between 10.0° N–10.0° S and the main accumulation regions located between 10.0° N–20.0° N and 10.0° S and 20.0° S.
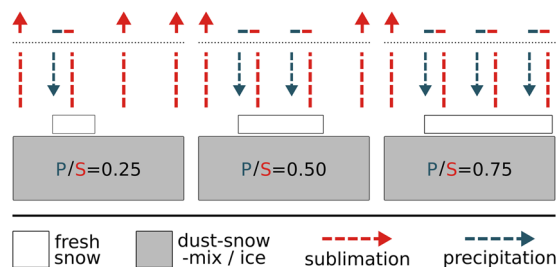

Fig. 4 Regenerative snow layer. Sublimation (S; dashed red lines), precipitation (P; dashed blue lines) fluxes, and the resulting fresh-snow-layer (white boxes) for three different P/S ratios. On short timescales the extent of a partial snow cover depends strongly on the orography and the near-surface winds. However, on longer timescales the snow cover converges to a state, in which the mass loss due to sublimation is balanced by the gain in mass due to snowfall. On an HSB, snow-covered as well as snow-free surfaces sublimate, while all precipitation adds to the snowpack. Thus, larger areas can exhibit a stable snow cover fraction even if overall sublimation exceeds precipitation. As long as temperatures stay below the melting point, the corresponding equilibrium extent is roughly proportional to the ratio of precipitation and sublimation. Thus, if precipitation is frequent enough, the surface will not be completely snow free, even in the ablation zones. In these regions, the net mass loss is proportional to sublimation from snow-free areas.

sustain deglaciation, as (sea) glacier flow from the accumulation zones would have been fast enough to balance the glacier degradation in the main ablation zone[28,47]. In the tropics, deglaciation is inhibited by an extensive, regenerative snow cover that prevents the albedo from decreasing to low enough values, even raising it with increasing pCO_2s. When more radiation is absorbed at the surface due to rising pCO_2s, sublimation and precipitation increase similarly and the P/S ratio remains very

high (Supplementary Fig. 2). Consequently, the intensification of the hydrological cycle does not lower the snow cover fraction—which remains steady at ~85–90% (Fig. 5c)—but increases the renewal rate of the snow at the top of the snowpack. This limits the aging process because it constrains snow grain growth and reduces the amount of dust that accumulates at the snowpack's surface. As a result of the increasingly short residence time of snow on the ground in combination with the large snow cover fraction, tropical surface albedos remain too high to initiate deglaciation and become increasingly independent of the dust accumulation rate and the properties of the material underlying the (fresh) snow layer.

In contrast, the simulated snow dynamics in the extratropics— between roughly 30° and 50°—allow for deglaciation well within a feasible pCO_2 range (Fig. 5b and Supplementary Fig. 3), and for extreme dust deposition rates snow and ice melt are simulated even at present-day pCO_2s (Fig. 6c). In the midlatitudes, the average sublimation and precipitation rates are lower than in the tropics, allowing more dust to accumulate on the snowpack. In addition, the daily-averaged solar irradiance peaks in the midlatitudes—during summer and winter, respectively—and the annual maximum temperatures are higher than in the tropics. The latter accelerate the snow aging process and the combination of large (near-) surface dust concentrations and high maximum temperatures results in albedos that are notably lower than in the tropics (compare Fig. 5a, b). Even the comparatively high peak snowfall rates at the onset of melting—of up to 20 mm month^{-1} —do not regenerate the snow cover fast enough to maintain a high enough surface albedo to prevent deglaciation (Fig. 6a, b). Furthermore, with maximum temperatures close to the melting point, an increase in surface net radiation does not increase sublimation but instead initiates snow and ice melt, with the meltwater draining from the surface without raising snowfall rates. Thus, for high dust deposition fluxes, the midlatitudes lack the snowfall-albedo feedback that dominates the tropics, resulting
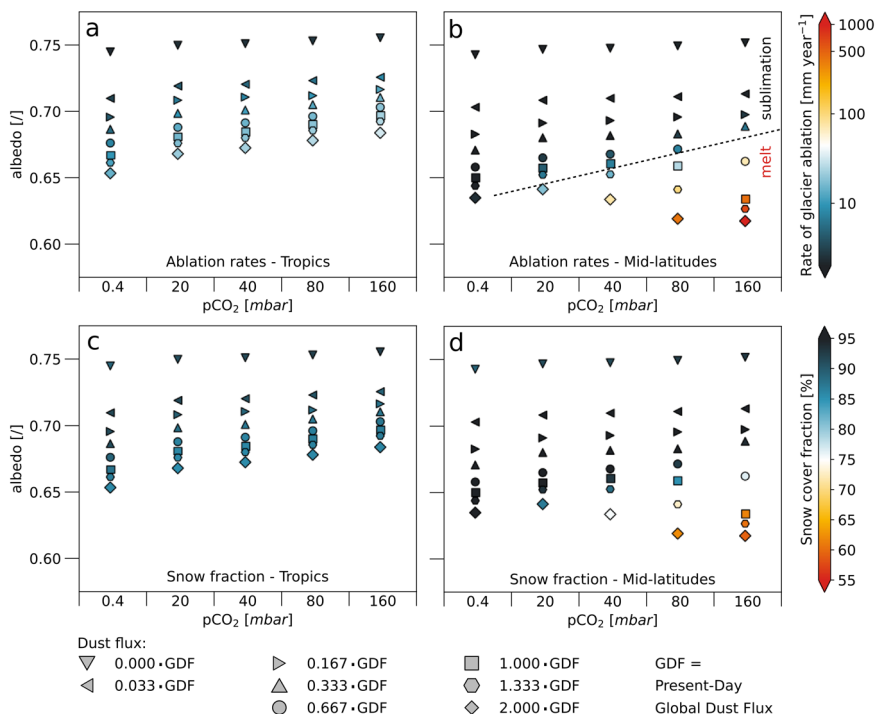
Fig. 5 Surface dynamics for varying dust deposition rates and CO₂ levels. **a** Simulated annual mean ablation rates in the tropical ablation zone as a function of pCO₂, prescribed dust deposition fluxes and the resulting annual mean albedo. The values are representative for a 18.75°-wide latitudinal band in the equatorial regions between roughly 10.0° N and 10.0° S. **b** Same as **a**, but showing values representative of a latitudinal band in the midlatitudes roughly between 30° S and 50° S. **c** Same as **a**, but showing the simulated annual mean snow cover. **d** Same as **b**, but showing the simulated annual mean snow cover. Symbols indicate the assumed dust deposition rates relative to the present-day global-mean dust flux (GDF): down-pointing triangle = no dust depositions, left-pointing triangle = 0.03 × GDF, right-pointing triangle = 0.16 × GDF, up-pointing triangle = 0.33 × GDF, circles = 0.66 × GDF, squares = GDF, hexagons = 1.33 × GDF, and diamonds = 2 × GDF. The simulations were carried out using the MPI-ESM1.2 (ref. [29]) with an adapted snow-albedo-scheme that estimates the albedo based on snow age and surface temperatures, and separates the snowpack into a top layer and a main layer ("Methods —Model configuration and Simulations"). Note that in subfigures **c** and **d**, an annual mean snow cover fraction of <75% indicates largely snow-free surfaces during several months in the snow melt season.
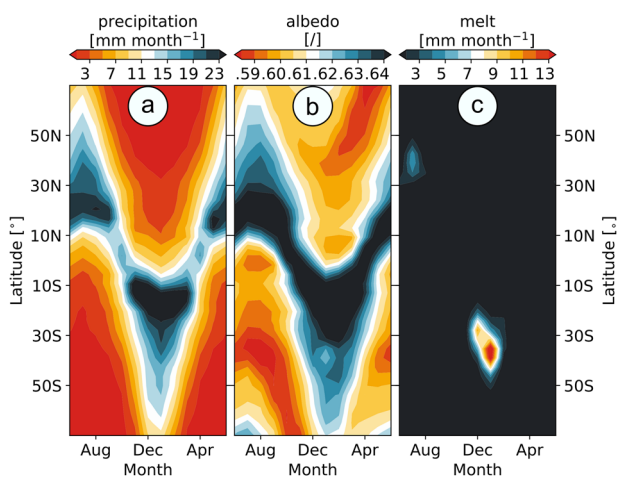

Fig. 6 Deglaciation for present-day atmospheric CO₂ concentrations. a Simulated zonal mean precipitation for dust deposition rates corresponding to 10 × present-day fluxes and atmospheric CO₂ concentrations of 0.4 mbar. **b** Same as **a**, but showing the simulated surface albedo. **c** Same as **a**, but showing melt rates.

in lower snow cover fractions and albedos for increasing pCO₂s. Here, the surface can even become snow free during parts of the melt season (Fig. 5d).

Under these circumstances, snow and ice melt are sustained for pCO₂s of 80 mbar when assuming present-day global-mean dust deposition rates (Fig. 5b), while a dust flux at 10× the present-day levels triggers melt even for present-day pCO₂s (Fig. 6c). As meltwater drains without affecting precipitation, the planet's ice cover is not necessarily in an equilibrium, in which lateral flow balances ice loss in the ablation zones. Thus, even the comparatively small melt fluxes that are simulated for pCO₂s of <100 mbar and present-day dust fluxes could have degraded the ice cover in the extratropics, triggering the deglaciation of an HSB. Moreover, the degradation could have progressed much more rapidly than our simulations indicate, as our model neglects a number of key processes associated with the melting of ice and snow. Our setup assumes all meltwater to drain from the surface immediately, while, in reality, it is more likely that liquid water would have formed puddles, ponds, lakes and connected stream networks before running off from the surface. Once melt is triggered, these would have lowered the albedo, initiating a positive feedback that could have accelerated local degradation processes substantially. For the assumption that standing water would not have drained at all, it has even been suggested that the formation of melt ponds in the midlatitudes could have warmed the planet to a point at which tropical temperatures hardly fall below the zero-degree-threshold and equatorial precipitation occurs (almost) exclusively in the form of rain. At this point, the snowfall-albedo feedback in tropical latitudes breaks down inducing a rapid degradation of the ice cover[53]. However, it is debatable whether midlatitude melt ponds could have raised large-scale temperatures on a fully glaciated planet notably beyond the melting point, as most of the excess energy would

have been consumed by the phase transition of ice and snow. This would require entire regions to have been largely covered by meltwater, which is a similarly extreme assumption as all meltwater draining from the surface instantly—and even then, the turbulent exchange in the boundary layer and small-scale circulations between the inundated and non-inundated areas would have likely maintained the average temperatures close to the melting point. As our model does not explicitly represent the effects of melt ponds, we can not assess how the deglaciation would have progressed once it was triggered. From a slow degradation of the midlatitude ice cover at comparatively low pCO_2s and temperatures to a rapid warming that triggers a degradation of ice sheets across a wide latitudinal range, many deglaciation trajectories are conceivable. An investigation of the deglaciation process will require not only an improved snow-albedo-scheme—as proposed in the present study—but also a scheme for melt ponds, as well as fully coupled sea ice and ice-sheet models.

Finally, it should be noted that we assumed melting to start at 0° C, which may be an overly conservative estimate. When sea ice sublimates, it is plausible that salt accumulates at the surface, lowering the melting point substantially[37]. Thus, the positive feedback due to the formation of surface-water bodies, and hence deglaciation, could have been triggered at lower CO_2 concentrations than estimated in this study. In general, the CO_2-threshold of deglaciation is very sensitive to a number of parameterizations used in the model and our simulations can only provide order-of-magnitude estimates rather than exact values. Here, we were conservative in the setup of our simulations, especially with respect to the albedo of snow and ice, as well as the treatment of meltwater ("Methods—Model configuration"), to not overestimate the potential of HSB deglaciation. Furthermore, the present version of the MPI-ESM possesses a comparatively low climate sensitivity amongst the CMIP6 participants[54,55]. The high climate sensitivity of some of the CMIP6-models may be an overestimation[56]; in contrast, the MPI-ESM is among the best models in reproducing observed temperature trends[57]. Nonetheless, it is likely that the pCO_2-threshold for deglaciation is—to a degree—model dependent, and that a higher climate sensitivity or lower snow and ice albedos reduce the pCO_2s required for deglaciation, which would make HSB deglaciation even more plausible.

Origin of high dust depositions. What, on a completely ice-covered planet, could have been the origin of the high dust fluxes required to trigger deglaciation? Volcanism provides one dust source that would have been present even on an HSB, and postglacial mantle decompression could have increased volcanic activity substantially[58,59]. However, this would serve only as a feedback subsequent to the initiation of deglaciation. Another dust source could be from terrestrial areas that may have remained ice free[2,60]. The climatic conditions in these areas would likely have produced large eolian erosion rates, resulting in dust deposition fluxes similar to those of the last glacial maximum, which were likely an order-of-magnitude larger than present-day fluxes[61,62]. Finally, though it may not have triggered the terminal deglaciation, ablation in the tropics would still have presented an effective mechanism to retain dust within a layer at the top of the planet's ice and snow cover[32,33]. With sublimation drying any exposed areas of such a dust layer, it would have been highly prone to eolian erosion, providing a regenerative source for advective dust transport into the midlatitudes.

The idea that deglaciation started in the midlatitudes due to erosion-induced dust redistribution, has important consequences for the geological evidence that can be expected from the deglaciation process. If an HSB existed and its deglaciation was triggered by the accumulation of a thick tropical dust layer, large bursts of material would have been flushed into the equatorial ocean and the resulting clay layers should be a common feature beneath the cap carbonates in the tropical ablation zones[30]. However, if the dust was constantly redistributed, the (near-) surface concentrations would have been lower, more uniform across the latitudes and would not have lead to distinguishable depositions upon deglaciation. Thus, a widespread presence of clay layers exclusively in the tropical ablation zone would provide strong evidence against the deglaciation history proposed in the present study. The observational record is far from conclusive; however, most of the known (paleo-) tropical snowball Earth field sites do not feature clay deposits at the glacial–postglacial boundary, while carbonate topped clay layers have been observed as far poleward as (roughly) 45° (Supplementary Fig. 4 and Supplementary Table 1). Thus, while the observations can not confirm a deglaciation that started in the midlatitudes, they do not disprove our hypothesis. Further, a spatially variable deglaciation could manifest in a unique sea-level rise fingerprint, observable in the succession of sediments that preserve the deglaciation. Though few sea-level curves for the deglaciation have been published, tropical sites often show an immediate transgression. In contrast, extra-tropical sites appear to record an initial regression, not necessarily unique to but consistent with deglaciation starting in the midlatitudes and progressing to the tropics (Supplementary Fig. 5). A number of factors will modify when and where sea-level rises during the deglaciation—including the length of the deglaciation and the size of the continental ice sheets, among other factors—and the geological evidence is far from conclusive. However, additional work constraining the relative timing of transgressive and regressive sequences may be able to test the hypotheses put forward here.

The modeling results presented here suggest that escape from an HSB is possible within a reasonable range of atmospheric CO_2, demonstrating that the theoretical implausibility of an HSB deglaciation is no longer a reason to reject such a possibility in Earth history. These results also hold implications for other solar systems—the outer-edge of the habitable zone, for example, is characterized by snowball-like states on rocky, water-rich planets[63]. Depending upon the tectonic mode of the planet and its volcanic CO_2 rates, the potential for a midlatitude deglaciation—shown by our result—may expand the outer limit upon which life-bearing planets can be found.

Methods

Model configuration. For our study, we used the land and the atmospheric component of the MPI-ESM1.2 (ref. [29]), the latest release of the Max-Planck-Institute for Meteorology's Earth system model. We ran these models in a terra-planet configuration with a global ice cover and in all grid boxes the land model is used to simulate the (near-) surface processes, with the parametrizations corresponding to those of glacier points. Thus, the setup does not account for the soil, bedrock, or ocean underlying the ice cover and the modeled surface consists of a 10-m-column of ice at the bottom of which a zero-flux condition is assumed. With the model configuration, we can simulate the complex atmospheric dynamics on a moderate spatiotemporal resolution with a reasonable amount of computational resources, as the simulated climate adapts to changes in the forcing comparatively quickly and the simulations come to an equilibrium within a spin-up period of <10 years.

Before giving a more detailed description of the modifications that were made to the MPI-ESM, it should be noted that our setup does not capture the entirety of the deglaciation-related processes, which would have required at least a sophisticated glacier- and coupled ocean-sea-ice model. Consequently, our approach has similar limitations as previous studies that relied on simulations with general circulation models[28] and the second part of our investigation, namely the feasibility of deglaciation, is only valid in the case that the overall behavior of the system is dominated by the processes modulating the snow albedo and cover. To confirm the applicability of our approach, we conducted a series of tests, in which we varied a number of key parameters, e.g., we prescribed an albedo of 0.4 for the ice underlying the snow layer in order to simulate the impact of a very dark surface similar to a thick dust layer that accumulated due to lateral glacier flow. Here, we

found that the snow-albedo-dynamics, and the respective feedbacks, indeed determine the behavior of the snowball system and while the ablation rates and deglaciation thresholds change slightly with varying parameters, the key findings remain unchanged, namely that the negative snow albedo feedback prohibits the onset of deglaciation in the tropics within the plausible CO_2 range, while deglaciation could have occurred in the extratropics, provided that dust fluxes were high enough. Furthermore, it should be noted that the atmospheric component shares certain shortcomings with other models which affect the performance at extreme atmospheric CO_2 concentrations[24]. For example, the radiation scheme does not account for the effects of pressure broadening on the opacity of the atmospheric greenhouse gases. However, within the geologically feasible CO_2 range, these effects would still have been comparatively small and even for the maximum CO_2 concentrations investigated in this study (400 mbar) neglecting them is still tolerable. In addition, for a spatially well mixed atmosphere, the respective effects would be similar for the tropics and the extratropics, hence they wouldn't change the main finding—that the onset of deglaciation would have occurred in the midlatitudes before it started in the tropics.

Our investigations did not require a great number of changes to the models' code and we ran them largely with the same parametrizations that are being used for the sixth phase of the Coupled Model Intercomparison Project[54]. One important exception pertains to the land component's snow-albedo-scheme, which we adapted to the specific requirements of a snowball Earth, and which we will describe in the following.

Snow-albedo-scheme. JSBACH, the land component of the MPI-ESM, employs two schemes to calculate the reflectivity of snow and the model's radiation scheme receives a weighted average of the resulting two albedos (usually an equal weight is applied)[64]. The first scheme is purely temperature based and in the range between -5 and $0\,°C$, the snow albedo decreases linearly between its maximum value—representing cold, dust-free snow—and its minimum value—representing snow containing dust at the melting point. Here, the snow albedos in the near-infrared α_{nir} and in the visible range α_{vis} are calculated as follows.

$$\alpha_{nir} = \alpha_{nir,min} + (\alpha_{nir,max} - \alpha_{nir,min}) \cdot \frac{T}{-5} \quad \text{for} -5 < T[°C] < 0, \text{ with} \quad (1)$$

$$\alpha_{nir,min} = 0.3 \quad \text{and} \quad (2)$$

$$\alpha_{nir,max} = 0.7 \quad \text{and} \quad (3)$$

$$\alpha_{vis} = \alpha_{vis,min} + (\alpha_{vis,max} - \alpha_{vis,min}) \cdot \frac{T}{-5} \quad \text{for} -5 < T[°C] < 0, \text{ with} \quad (4)$$

$$\alpha_{vis,min} = 0.5 \quad \text{and} \quad (5)$$

$$\alpha_{vis,max} = 0.9. \quad (6)$$

The second scheme calculates the snow albedo depending on the snow age, which is a function of the duration the snow has been on the ground, the snowfall rate, the surface temperature, and the dust deposition rate. Here, the albedo reduction due to the snow age f_{age} is described by the following function:

$$f_{age} = f_{age,max} \cdot \frac{\tau_{age}}{1 + \tau_{age}} \quad (7)$$

where $f_{age,max}$ constitutes the maximum albedo decrease due to aging, given by:

$$f_{age,max,nir} = 0.5 \quad \text{for the near infrared range, and} \quad (8)$$

$$f_{age,max,vis} = 0.3 \quad \text{for the visible range.} \quad (9)$$

τ_{age} represents the snow age which increases during a timestep Δt according to the following function:

$$\Delta\tau_{age} = (\tau_T + \min(\tau_T^{10}, 1) + \tau_D)\frac{\Delta t}{\tau_t} \quad (10)$$

where τ_T represents temperature effects on snow grain growth, τ_D effects of dust accumulation and τ_t a scaling factor:

$$\tau_T = \exp\left[5000\left(\frac{1}{t_{melt}} - \frac{1}{t_{surf}}\right)\right] \quad \text{and} \quad (11)$$

$$\tau_D = 0.3 \quad \text{for present} - \text{day dust depositions, and} \quad (12)$$

$$\tau_t = 10^6. \quad (13)$$

Note that, in the standard model, snowfall decreases the snow age. However, in the snow-albedo-scheme used in this study (see below) this term is no longer needed, hence we do not provide the respective equations here.

The main shortcoming of the MPI-ESM's snow-albedo-scheme lies in the fact that it treats the properties of snow at the surface as vertically uniform, and derives the albedo based on the characteristics of the entire snowpack, while in reality the snow albedo is determined only by the near-surface (usually only a few centimetres) snow

characteristics. Treating the snow cover as vertically uniform is the most common approach in large-scale models, including the ones that were used in previous snowball studies[28,32,33,49]; however, this is especially problematic for a snowball setup in which large areas on the globe retain a thick, perennial snow cover.

For the second set of simulations, we adapted the snow-albedo-scheme and separated the snowpack into a main layer and a top layer, each possessing its own thickness, cover fraction, age, and albedo. Falling snow is added to the top layer, increasing the layer's thickness, cover fraction, which is a function of the snow depth, and albedo while reducing the layer's age. The main layer's characteristics, however, are not affected by new snow. In our scheme, we assume that the top layer forms above the main layer and that the top layer's cover fraction is necessarily smaller than that of the main layer. This allows us to calculate the two layer's contributions to melt, sublimation and surface (mean) albedo simply by the fraction of the layer that is exposed to the atmosphere relative to the snow-covered fraction. Whenever the top layer covers >95% of the main layer, the snow contained in the top layer is added to the main layer, increasing the latter's albedo, depth and cover fraction (if not already at 100%), while decreasing its age. After the top layer has been added to the main layer or has disappeared as a result of ablation, a new top layer, which is initiated with the albedo corresponding to that of fresh snow and a zero age, forms whenever there is fresh snowfall. The result is a thick darker main layer whose extent is relatively stable and whose albedo continuously decreases (to the point when the snow contained in the top layer is added or the minimum albedo is reached), on top of which a thin, brighter top layer is located, whose extent and albedo quickly varies depending on snowfall, melt, and sublimation rates.

Dust deposition rates are one of the key factors determining the snow albedo, but our model setup does not allow us to explicitly account for the factors that determine the respective fluxes. Dust particles are not a standard tracer in the atmospheric component of the model, but most importantly explicitly modeling dust sources on an ice-covered planet, such as volcanic eruptions, potentially exposed terrestrial areas or a tropical surface dust layer, goes beyond the scope of this study and the abilities of our model. Consequently, we prescribe globally uniform dust deposition rates (as is the current standard in the MPI-ESM) and use them as an input variables similar to the atmospheric CO_2 concentrations. More precisely we prescribe τ_D in Eq. (10)—e.g., 0.3 for present-day dust fluxes and 0.6 for a doubling of the dust depositions.

In JSBACH, the dust concentrations within the snowpack are not simulated explicitly and the impact of impurities is only accounted for in the snow's age and represented by a factor for the dust deposition rates in the respective calculations. Thus, in order to simulate the effect of dust accumulation due to ablation, we allow the main layer to age at the same rate as the top layer, even though the main layer is not (fully) exposed to the surface dust deposition flux as it is (partly) covered by the top layer. Consequently, whenever the top layer disappears, as a result of snow melt or sublimation, and more of the main layer is exposed, the main layer has already received the same amount of dust as was embedded in the top layer and has aged accordingly. Here, it should be noted that this approach potentially overestimates the dust accumulation under the circumstances that ablation is mainly the result of melt. Whenever ablation is driven by sublimation, it can be assumed that the embedded particles remain at the surface, darkening the underlying snow, but when temperatures reach the melting point it is unclear how much of the dust would remain on top of the snowpack and which fraction would be washed away with the meltwater[33]. However, even the assumption that all the dust would be washed away with the meltwater would not change our results fundamentally. This is because the simulated melt rates are so large that melt does not only degrade the top layer, but also reduces the main layer substantially and in most simulations, in which melt is triggered the snow cover largely disappears during the snow melt season. And under the circumstances that also the main layer disappears it is assumed that the dust is removed from the surface.

Besides these major structural changes, we made some minor adaptations mostly in the form of parameter modifications. Instead of using the weighted average of the temperature- and the age-based snow albedo, we use the minimum of the two, but at the same time we raised the maximum albedo of fresh snow to 0.95 for visible and 0.75 for near-infrared radiation. In addition, we changed the threshold above which the snow albedo is sensitive to surface temperature from -5 to $-1\,°C$ (corresponding to the temperature threshold employed for snow-covered sea ice in MPIOM, the MPI-ESM's ocean component), but at the same time, we changed the formulation so that increasing temperatures can only lower the albedo, while decreasing temperatures do not increase it. Furthermore, we removed the factor representing the snowfall rate from the snow age calculation. This was done because our scheme is designed in a way that snowfall does not affect the characteristics of the main layer, while the characteristics of the top layer are calculated as a weighted average (based on the snow water equivalent) between the snow within the top layer and the snow that falls within any given timestep. The latter is possible because the top layer is necessarily so thin that the entire snow contained within the layer has an effect on the layer's optical properties.

Finally, it should be noted that we prescribe the ice albedo and, as a consequence, we neglect certain processes which lower the ice albedo in the ablation regions. Most importantly, we do not consider the effect of melt ponds and lakes on the albedo, as the meltwater flux in JSBACH is immediately removed from the surface. With seasonal meltwater fluxes of several hundred mm, the resulting puddles, ponds and lakes would substantially darken the surface before draining from the ice cover. This would have increased the amount of absorbed radiation,

raising surface temperatures, which in turn promotes the extension and formation of ponds. The presence of standing water would have also lowered the impact of fresh snow on the surface albedo, weakening the snowfall-albedo feedback. Furthermore, an accumulation of salt could have lowered the freezing point, which would have lead to the formation of surface-water bodies at sub-zero temperatures. However, simulating the mechanisms that lead to standing water at the surface of a snowball Earth is beyond the capabilities of most large-scale models and we are only aware of one attempt, by Wu et al.[53], to explicitly account for the formation of melt ponds. Here, one major problem is the uncertainty with respect to the drainage of these ponds, which could happen extremely fast once connected flow pathways have formed. Another problem is the estimation of the spatial extent of inundated areas, which strongly depends on the small (subgrid) scale orography. Wu et al. deal with the respective uncertainties, by assuming that there is no drainage of meltwater (even though they limit the maximum pond depth) and by determining the area of melt ponds purely based on a subgrid scale distribution of the surface temperatures. Here, the assumption is that, even below the melting point, random temperature fluctuations can trigger melt, while negative deviations do not cause an immediate refreezing of liquid water. This, allows melt ponds to persist at sub-zero temperatures, covering up to 80% of the grid cell before temperatures reach the melting point. These assumptions are no less extreme than neglecting melt ponds altogether, but risk an overestimation of the respective impact on the deglaciation process. For the present study, we decided not to include the above effects of melt ponds for the following reason. The formation of surface-water bodies provides a positive feedback that necessarily raises the likelihood of deglaciation—once melting is triggered—and the uncertainty involved in the respective parametrizations only increases the risk of overestimating the potential for exiting the icehouse state. Thus, the most robust estimation of the deglaciation potential is obtained by neglecting all of the above processes.

Another shortcoming of our model is that we only account for the accumulation of dust within the snowpack, but not at the snow-ice-interface. Whenever the snowpack is completely melted, the dust is assumed to be washed away completely. However, when snow and ice melt in reality, a given fraction of the dust is not washed away with the runoff and drained from the surface, but may remain behind, e.g., within cryoconite holes[2,33]. It is exceedingly difficult to estimate the fraction of dust that would remain behind after the melting period and how long the cryoconite holes could last before they also drain, as this is determined by a variety of factors that we do not account for in the model. To counteract the absence of these effects in the model, we prescribe a comparatively low surface albedo, i.e., 0.53, that best represents sea ice, even though the near-surface ice would most likely have consisted of brighter meteoric ice[33,35,65]. Here, it can be argued, that sea ice, especially when partly covered in dust, would have had an even lower albedo. Similar arguments can be made about our minimum snow albedo of ~0.59[35]. In fact, we performed explorative simulations, in which we set these parameters to the lower end of the plausible range. This decreased the simulated deglaciation thresholds, but did not change the outcome that deglaciation would have been triggered in the extra—rather than in the tropics. Nonetheless, for the study, we only used simulations with higher albedo values to ensure that our findings are valid for a broader range of assumptions—that is not only for albedo values at the lower end of the plausible range.

This complex approach to determine the albedo was only required for the second set of simulations ("Thawing the snowball") and for the first set ("Dependency of ablation rates on albedo and CO_2") we simply included the option to prescribe a fixed albedo value for the snow cover, as well as for the underlying ice. This allowed us to set the overall surface albedo independent of the simulated snow dynamics.

Simulations. In all simulations, the model was run using a temporal resolution of 450 s and a vertical resolution of 47 atmospheric model levels and 5 vertical subsurface layers. The horizontal resolution of the simulations was T31 (3.75° × 3.75°), which corresponds to a grid-spacing of ~415 km in tropical latitudes. To facilitate the comparability of our results, the setup of our simulations is very similar to that of previous studies, in that we removed the orography and reduced the solar constant to 94% of its present-day value[28]. Note that otherwise the orbital parameters were prescribed using present-day values.

For the first set of experiments, we initiated the model with an pCO_2 of 0.4 mbar and an ice-covered but snow-free surface. During the 10-year spin-up period, in which we gradually reduced the orography, the state of the atmosphere, (sub-) surface temperatures and precipitation rates adapted very quickly to the prescribed surface albedo and a complete snow cover was established (note that in the first set of simulations the snow cover has no effect on the surface albedo). After the spin-up period, we ran the model for a 100-year-period during which we gradually increased the pCO_2 to 400 mbar. For the second set of experiments, we started our simulations from the states that were simulated at the end of the spin-up period for a prescribed surface albedo of 0.66. Here, we removed the snow cover and ran the simulations for a 20-year period with a constant pCO_2 of 0.4 mbar, an ice albedo of 0.53 and the snow-albedo-dynamics, resulting from a given dust deposition rate. The first 10 years of this period were required for the snow cover and the surface albedo to come to an equilibrium and the second 10 years were used in the analysis. After this period, we removed the snow cover, increased the CO_2 concentration, and continued the simulation for another 20 years, again with 10 years required for

the atmosphere and the surface to adapt to the increase in CO_2 concentrations. These steps were repeated until CO_2 levels of 160 mbar were reached (with intermediate CO_2 concentrations of 20, 40, and 80 mbar).

Data availability

Code availability

References

1. Kirschvink, J. L. in *The Proterozoic Biosphere: a Multidisciplinary Study*, Chp. 2.3, 51–52 (Cambridge University Press, 1992).
2. Hoffman, P. F. et al. Snowball earth climate dynamics and cryogenian geology-geobiology. *Sci. Adv.* **3**, e1600983 (2017).
3. Evans, D. A., Beukes, N. J. & Kirschvink, J. L. Low-latitude glaciation in the Palaeoproterozoic era. *Nature* **386**, 262–266 (1997).
4. Hoffman, P. F., Halverson, G. P., Schrag, D. P. & Kaufman, A. J. A neoproterozoic snowball earth. *Science* **281**, 1342–1346 (1998).
5. Macdonald, F. A. et al. Calibrating the cryogenian. *Science* **327**, 1241–1243 (2010).
6. Evans, D. A. D. & Raub, T. D. Chapter 7 neoproterozoic glacial palaeolatitudes: a global update. *Geol. Soc. Lond. Mem.* **36**, 93–112 (2011).
7. Li, Z.-X., Evans, D. A. & Halverson, G. P. Neoproterozoic glaciations in a revised global palaeogeography from the breakup of rodinia to the assembly of gondwanaland. *Sediment. Geol.* **294**, 219–232 (2013).
8. Rooney, A. D., Strauss, J. V., Brandon, A. D. & Macdonald, F. A. A cryogenian chronology: two long-lasting synchronous neoproterozoic glaciations. *Geology* **43**, 459–462 (2015).
9. Bruce, R. Loophole for snowball Earth. *Nature* **405**, 403–404 (2000).
10. Olcott, A. N. Biomarker evidence for photosynthesis during neoproterozoic glaciation. *Science* **310**, 471–474 (2005).
11. Richard, P. W., Yonggang, L. & Crowley, J. W. Snowball Earth prevention by dissolved organic carbon remineralization. *Nature* **450**, 813 (2007).
12. Allen, P. A. & Etienne, J. L. Sedimentary challenge to Snowball Earth. *Nat. Geosci.* **1**, 817–825 (2008).
13. Ghil, M. Climate stability for a sellers-type model. *J. Atmos. Sci.* **33**, 3–20 (1976).
14. Marotzke, J. & Botzet, M. Present-day and ice-covered equilibrium states in a comprehensive climate model. *Geophys. Res. Lett.* **34**, L16704 (2007).
15. Ferreira, D., Marshall, J. & Rose, B. Climate determinism revisited: multiple equilibria in a complex climate model. *J. Clim.* **24**, 992–1012 (2011).
16. Voigt, A. & Abbot, D. S. Sea-ice dynamics strongly promote snowball earth initiation and destabilize tropical sea-ice margins. *Clim. Past* **8**, 2079–2092 (2012).
17. Amber, W., Thomas, B. & M., S. D. Extreme sensitivity in Snowball Earth formation to mountains on PaleoProterozoic supercontinents. *Sci. Rep.* **9**, 2349 (2019).
18. Hyde, W. T., Crowley, T. J., Baum, S. K. & Richard, P. W. Neoproterozoic 'snowball Earth' simulations with a coupled climate/ice-sheet model. *Nature* **405**, 425–429 (2000).
19. Lewis, J. P., Weaver, A. J. & Eby, M. Snowball versus slushball earth: Dynamic versus nondynamic sea ice? *J. Geophys. Res. Oceans* **112**, C11014 (2007).
20. Abbot, D. S., Voigt, A. & Koll, D. The jormungand global climate state and implications for neoproterozoic glaciations. *J. Geophys. Res. Atmos.* **116**, D18103 (2011).
21. Pierrehumbert, R., Abbot, D., Voigt, A. & Koll, D. Climate of the neoproterozoic. *Annu. Rev. Earth Planet. Sci.* **39**, 417–460 (2011).
22. Rose, B. E. J. Stable "waterbelt" climates controlled by tropical ocean heat transport: a nonlinear coupled climate mechanism of relevance to snowball earth. *J. Geophys. Res. Atmos.* **120**, 1404–1423 (2015).
23. Pierrehumbert, R. T. High levels of atmospheric carbon dioxide necessary for the termination of global glaciation. *Nature* **429**, 646–649 (2004).
24. Pierrehumbert, R. T. Climate dynamics of a hard snowball earth. *J. Geophys. Res. Atmos.* **110**, D01111 (2005).

25. Hir, G. L., Ramstein, G., Donnadieu, Y. & Pierrehumbert, R. T. Investigating plausible mechanisms to trigger a deglaciation from a hard snowball earth. *C. R. Geosci.* **339**, 274–287 (2007).

26. Abbot, D. S. et al. Clouds and snowball earth deglaciation. *Geophys. Res. Lett.* **39**, L20711 (2012).

27. Hu, Y., Yang, J., Ding, F. & Peltier, W. Model-dependence of the co 2 threshold for melting the hard snowball earth. *Clim. Past* **7**, 17–25 (2011).

28. Abbot, D. S. et al. Robust elements of snowball earth atmospheric circulation and oases for life. *J. Geophys. Res. Atmos.* **118**, 6017–6027 (2013).

29. Mauritsen, T. et al. Developments in the mpi-m earth system model version 1.2 (mpi-esm1.2) and its response to increasing co2. *J. Adv. Model. Earth Syst.* **11**, 998–1038 (2019).

30. Abbot, D. S. & Pierrehumbert, R. T. Mudball: surface dust and snowball earth deglaciation. *J. Geophys. Res.* **115**, D03104 (2010).

31. Hir, G. L., Donnadieu, Y., Krinner, G. & Ramstein, G. Toward the snowball earth deglaciation…. *Clim. Dyn.* **35**, 285–297 (2010).

32. Li, D. & Pierrehumbert, R. T. Sea glacier flow and dust transport on snowball earth. *Geophys. Res. Lett.* **38**, L17501 (2011).

33. Goodman, J. C. & Strom, D. C. Feedbacks in a coupled ice-atmosphere-dust model of the glacial neoproterozoic "mudball earth". *J. Geophys. Res. Atmos.* **118**, 11,546–11,557 (2013).

34. Brandt, R. E., Warren, S. G., Worby, A. P. & Grenfell, T. C. Surface albedo of the antarctic sea ice zone. *J. Clim.* **18**, 3606–3622 (2005).

35. Dadic, R., Mullen, P. C., Schneebeli, M., Brandt, R. E. & Warren, S. G. Effects of bubbles, cracks, and volcanic tephra on the spectral albedo of bare ice near the transantarctic mountains: implications for sea glaciers on snowball earth. *J. Geophys. Res. Earth Surf.* **118**, 1658–1676 (2013).

36. Zatko, M. C. & Warren, S. G. East antarctic sea ice in spring: spectral albedo of snow, nilas, frost flowers and slush, and light-absorbing impurities in snow. *Ann. Glaciol.* **56**, 53–64 (2015).

37. Light, B., Carns, R. C. & Warren, S. G. The spectral albedo of sea ice and salt crusts on the tropical ocean of snowball earth: 1. laboratory measurements. *J. Geophys. Res. Oceans* **121**, 4966–4979 (2016).

38. Lewis, J. P., Weaver, A. J. & Eby, M. Deglaciating the snowball earth: sensitivity to surface albedo. *Geophys. Res. Lett.* **33**, L23604 (2006).

39. Fountain, A. G., Jacobel, R. W., Schlichting, R. & Jansson, P. Fractures as the main pathways of water flow in temperate glaciers. *Nature* **433**, 618–621 (2005).

40. Das, S. B. et al. Fracture propagation to the base of the greenland ice sheet during supraglacial lake drainage. *Science* **320**, 778–781 (2008).

41. Krawczynski, M. J., Behn, M. D., Das, S. B. & Joughin, I. Constraints on the lake volume required for hydro-fracture through ice sheets. *Geophys. Res. Lett.* **36**, L10501 (2009).

42. Simkins, L. M. et al. Anatomy of a meltwater drainage system beneath the ancestral East Antarctic ice sheet. *Nat. Geosci.* **10**, 691–697 (2017).

43. Smith, L. C. et al. Direct measurements of meltwater runoff on the greenland ice sheet surface. *Proc. Natl Acad. Sci.* **114**, E10622–E10631 (2017).

44. Huiming, B., Lyons, J. R. & Chuanming, Z. Triple oxygen isotope evidence for elevated CO2 levels after a Neoproterozoic glaciation. *Nature* **453**, 504–506 (2008).

45. Wiscombe, W. J. & Warren, S. G. A model for the spectral albedo of snow. i: Pure snow. *Journal of the Atmos. Sci.* **37**, 2712–2733 (1980).

46. Dang, C., Fu, Q. & Warren, S. G. Effect of snow grain shape on snow albedo. *J. Atmos. Sci.* **73**, 3573–3583 (2016).

47. Goodman, J. C. & Pierrehumbert, R. T. Glacial flow of floating marine ice in "snowball earth". *J. Geophys. Res. Oceans* **108**, 3308 (2003).

48. Hoffman, P. F. & Schrag, D. P. Considering a neoproterozoic snowball earth: reply. *Science* **284**, 1087–1087 (1999).

49. Pollard, D., Kasting, J. F. & Zugger, M. E. Snowball earth: asynchronous coupling of sea-glacier flow with a global climate model. *J. Geophys. Res. Atmos.* **122**, 5157–5171 (2017).

50. Roesch, A., Wild, M., Gilgen, H. & Ohmura, A. A new snow cover fraction parametrization for the echam4 gcm. *Clim. Dyn.* **17**, 933–946 (2001).

51. Roesch, A. & Roeckner, E. Assessment of snow cover and surface albedo in the echam5 general circulation model. *J. Clim.* **19**, 3828–3843 (2006).

52. Dadic, R., Mott, R., Lehning, M. & Burlando, P. Wind influence on snow depth distribution and accumulation over glaciers. *J. Geophys. Res. Earth Surf.* **115**, F01012 (2010).

53. Wu, J., Liu, Y. & Zhao, Z. How should snowball earth deglaciation start. *J. Geophys. Res. Atmos.* **126**, e2020JD033833 (2021).

54. Eyring, V. et al. Overview of the coupled model intercomparison project phase 6 (CMIP6) experimental design and organization. *Geosci. Model Dev.* **9**, 1937–1958 (2016).

55. Zelinka, M. D. et al. Causes of higher climate sensitivity in CMIP6 models. *Geophys. Res. Lett.* **47**, e2019GL085782 (2020).

56. Zhu, J., Poulsen, C. J. & Otto-Bliesner, B. L. High climate sensitivity in CMIP6 model not supported by paleoclimate. *Nat. Clim. Change* **10**, 378–379 (2020).

57. Beusch, L., Gudmundsson, L. & Seneviratne, S. I. Crossbreeding CMIP6 earth system models with an emulator for regionally optimized land temperature projections. *Geophys. Res. Lett.* **47**, e2019GL086812 (2020).

58. Mason, B. G., Pyle, D. M. & Oppenheimer, C. The size and frequency of the largest explosive eruptions on earth. *Bull. Volcanol.* **66**, 735–748 (2004).

59. Huybers, P. & Langmuir, C. Feedback between deglaciation, volcanism, and atmospheric co2. *Earth Planet. Sci. Lett.* **286**, 479–491 (2009).

60. Ewing, R. C. et al. New constraints on equatorial temperatures during a late neoproterozoic snowball earth glaciation. *Earth Planet. Sci. Lett.* **406**, 110–122 (2014).

61. Claquin, T. et al. Radiative forcing of climate by ice-age atmospheric dust. *Clim. Dyn.* **20**, 193–202 (2003).

62. Abbot, D. S. & Halevy, I. Dust aerosol important for snowball earth deglaciation. *J. Clim.* **23**, 4121–4132 (2010).

63. Abbot, D. S. Analytical investigation of the decrease in the size of the habitable zone due to a limited co2 outgassing rate. *Astrophys. J.* **827**, 117 (2016).

64. Engels, J. *The Impact of Black Carbon Aerosol Induced Snow Darkening on the Radiation Balance in ECHAM6: Quantifying the Contribution of Wildfires for Present and Future Conditions*. Ph.D. thesis, Universität Hamburg Hamburg (2016).

65. Goodman, J. C. Through thick and thin: marine and meteoric ice in a "snowball earth" climate. *Geophys. Res. Lett.* **33**, L16701 (2006).

Author contributions

P.d.V. designed the experiments, performed model adaptations, conducted simulations, and analysis and prepared the manuscript. T.S. performed model adaptations and was involved in the analysis. J.C.R. and J.G. analyzed the observational evidence. V.B. contributed to the analysis and the preparation of the manuscript. All authors reviewed and contributed to the manuscript.

Funding

Competing interests

The authors declare no competing interests.

Additional information